Received: 1 June 2023 | Accepted: 2 June 2023 | Published on: 19 June 2023

DOI: 10.1002/asna.20230095

Astronomische Nachrichten

PROCEEDING

Neutrino physics: Experimental and theoretical challenges

Ricardo González Felipe[1,2]

[1]ISEL–Instituto Superior de Engenharia de Lisboa, Instituto Politécnico de Lisboa, Lisboa, Portugal

[2]CFTP–Centro de Física Teórica de Partículas, Instituto Superior Técnico, Universidade de Lisboa, Lisboa, Portugal

Correspondence
Ricardo González Felipe, ISEL–Instituto Superior de Engenharia de Lisboa, Instituto Politécnico de Lisboa, Rua Conselheiro Emídio Navarro, 1959-007, Lisboa, Portugal.
Email: ricardo.felipe@isel.pt

Funding information
Fundação para a Ciência e a Tecnologia, Grant/Award Numbers: CERN/FIS-PAR/0019/2021, CFTP-FCT Unit UIDB/00777/2020, UIDP/00777/2020

The existence of massive neutrinos is the first solid evidence of physics beyond the standard model of particle physics. A remarkable progress has been achieved in solar, atmospheric, reactor, and accelerator neutrino experiments during the last decades. On the theoretical side, several questions are being addressed, namely the Dirac or Majorana nature of neutrinos, the mechanisms for neutrino mass generation, and the relation between neutrinos and the matter–antimatter asymmetry observed in the Universe, among others. This article provides a brief overview on some of the current experimental and theoretical aspects in neutrino physics.

KEYWORDS
neutrino oscillations, seesaw mechanism, leptogenesis, flavor symmetries

1 | INTRODUCTION

Neutrinos were postulated by Wolfgang Pauli more than 90 years ago and discovered almost 70 years ago at the Cowan–Reines experiment (Cowan et al. 1956). Since then, these elusive particles have attracted the attention of physicists, and many efforts have been made to shed light on the properties of neutrinos.

The observation of neutrino flavor oscillations, first at Homestake (Davis Jr. et al. 1968) and Super-Kamiokande (Fukuda et al. 1998) experiments, and then in several solar, atmospheric, reactor, and accelerator experiments, firmly establishes that neutrinos are massive particles. This provides the first direct evidence for the existence of physics beyond the standard model (SM). With the advent of a new precision era, upcoming and next-generation neutrino experiments will provide important clues to the still unanswered questions. In this article, we present a summary of some of the current experimental and theoretical challenges in the physics of neutrinos. The review is by no means complete and several aspects were necessarily left aside. The latter are covered in many books and review articles on neutrino physics available in the literature.

The article is organized as follows. Section 2 is devoted to review several aspects related to experimental searches in neutrino physics. In Section 2.1, we give an overview of the present status of neutrino oscillation parameters, based on global analyses of the available data from solar, atmospheric, reactor, and accelerator neutrino experiments. Laboratory experiments aiming at establishing the absolute neutrino mass scale are discussed in Section 2.2. A comparison with current astrophysical and cosmological constraints is also presented. In Section 2.3, we comment on scenarios beyond the standard three-neutrino (3ν) picture, namely on experimental hints and anomalies that have been reported and suggest the existence of eV-mass sterile neutrinos, as well as on theoretical motivations for introducing additional sterile neutrinos with masses at higher scales.

Section 3 is dedicated to discuss some of the outstanding problems in the theory of neutrinos. The particle nature of neutrinos is addressed in Section 3.1, while Section 3.2 is devoted to discuss viable mechanisms for the generation of neutrino masses. The possibility that neutrinos may have played a crucial role in the origin of the matter–antimatter asymmetry of the Universe is

considered in Section 3.3. Finally, in Section 3.4, different approaches to neutrino mass models are commented on. Our concluding remarks are given in Section 4.

2 | EXPERIMENTAL CHALLENGES

2.1 | Present status of neutrino oscillation parameters

If neutrinos are massive particles and lepton flavors mix in the weak charged-current interactions, flavor oscillations can occur when neutrinos propagate through space. The flavor state $|\nu_\alpha\rangle$ is created and detected as a coherent superposition of mass eigenstates $|\nu_i\rangle$ (Bilenky & Pontecorvo 1976a; Bilenky & Pontecorvo 1976b; Eliezer & Swift 1976; Fritzsch & Minkowski 1976), i.e.,

$$|\nu_\alpha\rangle = \sum_{i=1}^{n} U^*_{\alpha i}|\nu_i\rangle, \tag{1}$$

where n is the number of light neutrinos and U is the Pontecorvo–Maki–Nakagawa–Sakata (PMNS) lepton mixing matrix (Maki et al. 1962; Pontecorvo 1957), analogous to the Cabibbo–Kobayashi–Maskawa (CKM) matrix in the quark sector (Cabibbo 1963; Kobayashi & Maskawa 1973).

For three lepton generations, as it is the case of the SM, the unitary PMNS matrix can be parameterized in terms of three mixing angles and three CP-violating phases in the form

$$U = \begin{pmatrix} c_{12}c_{13} & s_{12}c_{13} & s_{13} \\ -s_{12}c_{23} - c_{12}s_{23}s_{13}e^{i\delta} & c_{12}c_{23} - s_{12}s_{23}s_{13}e^{i\delta} & s_{23}c_{13}e^{i\delta} \\ s_{12}s_{23} - c_{12}c_{23}s_{13}e^{i\delta} & -c_{12}s_{23} - s_{12}c_{23}s_{13}e^{i\delta} & c_{23}c_{13}e^{i\delta} \end{pmatrix} \times \begin{pmatrix} 1 & 0 & 0 \\ 0 & e^{i\alpha_{21}/2} & 0 \\ 0 & 0 & e^{i\alpha_{31}/2} \end{pmatrix}, \tag{2}$$

where $c_{ij} = \cos\theta_{ij}$ and $s_{ij} = \sin\theta_{ij}$, with θ_{12}, θ_{13} and θ_{23} being the three mixing angles; δ is the Dirac CP phase and α_{21}, α_{31} denote the two Majorana phases.

Note that the above parameterization slightly differs from its CKM analogous, since the particle nature of neutrinos is presently unknown. If neutrinos were Dirac particles, the two Majorana phases would be unphysical and only the phase δ would remain, as in the case of the quark mixing matrix. In the case of Majorana neutrinos, all three phases are physical. Yet, only the Dirac phase δ can be probed in neutrino oscillation experiments.[1]

For all practical purposes, neutrinos that propagate in vacuum can be considered ultra-relativistic particles having the same momentum $p \gg m_i$ (m_i is the mass of the neutrino mass eigenstate $|\nu_i\rangle$). Thus, the energy E_i of each neutrino state can be approximated by $E_i = (p^2 + m_i^2)^{1/2} \simeq p + m_i^2/(2p)$. After travelling a distance $L \simeq t$ from the source to the detector, the flavor states evolve as

$$|\nu_\alpha(t)\rangle = U^*_{\alpha i} e^{-iE_i t}|\nu_i\rangle, \tag{3}$$

assuming the plane-wave approximation. The probability of detecting a neutrino with flavor β after a time t is thus given by Giunti & Kim (2007)

$$\begin{aligned} P(\nu_\alpha \to \nu_\beta) &= |\langle\nu_\beta|\nu_\alpha(t)\rangle|^2 = \left|\sum_{i,j} U^*_{\alpha i} U_{\beta j} e^{-iE_i t}\langle\nu_j|\nu_i\rangle\right|^2 \\ &= \delta_{\alpha\beta} - 4\sum_{i>j}\mathrm{Re}\left[U^*_{\alpha i}U_{\beta i}U_{\alpha j}U^*_{\beta j}\right]\sin^2\left(\frac{\Delta m^2_{ij}L}{4E}\right) \\ &\quad + 2\sum_{i>j}\mathrm{Im}\left[U^*_{\alpha i}U_{\beta i}U_{\alpha j}U^*_{\beta j}\right]\sin\left(\frac{\Delta m^2_{ij}L}{2E}\right), \end{aligned} \tag{4}$$

where, in the last expression, the orthogonality condition $\langle\nu_j|\nu_i\rangle = \delta_{ij}$ has been used, $\Delta m^2_{ij} = m^2_i - m^2_j$ is the mass-squared difference, and E is the neutrino energy.[2] A similar expression is obtained for the oscillation probability of antineutrinos propagating in vacuum, with the obvious substitution of U by its conjugate U^*. Therefore, for neutrinos and antineutrinos, the first term in the right-hand side of Equation (4) turns out to be the same (CP-conserving), while the last one has opposite signs (CP-violating).

In cases where the experimental results are well described by effective two-flavor oscillations, with a single mass-squared difference Δm^2 and an angle θ that parameterizes the neutrino mixing, Equation (4) takes the simplified form

$$P(\nu_\alpha \to \nu_\beta) = \delta_{\alpha\beta} - (2\delta_{\alpha\beta} - 1)\sin^2(2\theta)\sin^2\left(\frac{\Delta m^2 L}{4E}\right). \tag{5}$$

This is the case in solar neutrino experiments, where oscillation data can be well fitted taking into account only the mixing angle θ_{12} and the mass-squared splitting Δm^2_{21}.

Equation (4) shows that the oscillation probability P is sensitive to the mixing angles θ_{ij}, the Dirac CP phase δ, the neutrino mass-squared differences, and the distance L and energy E fixed in a given experiment. Notice however that no information on the absolute value of the neutrino masses and Majorana phases can be obtained

[1] Information on the Majorana phases can be obtained, for instance, in processes that violate lepton number such as $0\nu\beta\beta$ decay.

[2] Actually, neutrino oscillation experiments measure an average probability, since neutrino beams do not have a mono-energetic spectrum and detectors have a finite energy resolution.

from neutrino oscillation experiments. As far as CP violation is concerned, it can only be accessed in appearance experiments, since disappearance processes, which measure the survival probability $P(\nu_\alpha \to \nu_\alpha)$, are insensitive to CP-violating effects.

Several neutrino experiments are currently being performed to observe neutrino oscillations and others are being planned for the near future. Let us briefly comment on these experiments.

Solar experiments have the best sensitivity to constrain the mixing angle θ_{12} and the mass-squared splitting Δm^2_{21}. Current experiments include the liquid scintillator experiment Borexino (Alimonti et al. 2009), the water Cherenkov detector Super-Kamiokande (Abe et al. 2016), and the heavy-water experiment SNO+ (Albanese et al. 2021). The next-generation detector JUNO is under construction (An et al. 2016).

Atmospheric experiments are most sensitive to the mixing angle θ_{23} and the mass splitting Δm^2_{31}. Current experiments include Super-Kamiokande (Abe et al. 2018a), IceCube DeepCore (Aartsen 2018; Aartsen et al. 2019) and Antares (Albert et al. 2019). Among the future projects are Hyper-Kamiokande (Abe et al. 2018b), IceCube Upgrade (Ishihara 2021), and KM3NeT/ORCA (Aiello et al. 2022).

Reactor experiments are usually categorized as short baseline (SBL) and long baseline (LBL). SBL experiments, like RENO (Bak et al. 2018) and Daya-Bay (Adey et al. 2018), are sensitive to the mixing angle θ_{13} and to a mass splitting combination involving θ_{12}, Δm^2_{31}, and Δm^2_{32}, while the LBL experiment KamLAND (Abe et al. 2008; Gando et al. 2011) is more sensitive to θ_{12} and Δm^2_{21}. The new SBL experiments NEOS (Ko et al. 2017), DANSS (Alekseev et al. 2018), STEREO (Almazán et al. 2020), PROSPECT (Andriamirado et al. 2021), NEUTRINO-4 (Serebrov et al. 2021), and SoLid (Abreu et al. 2021) will be able to probe a mass splitting beyond the standard three active neutrino picture, with $\Delta m^2 \sim 1\ \text{eV}^2$.

Accelerator experiments can be classified as SBL and LBL. The current LBL accelerator experiments NOνA (Acero et al. 2019; Himmel 2020) and T2K (Abe et al. 2020; Dunne 2020) not only measure the mixing angle θ_{23} and the mass splitting Δm^2_{31}, but also are sensitive to θ_{13} and the Dirac phase δ. Future LBL experiments with improved sensitivity include Hyper-Kamiokande (T2HK) (Abe et al. 2018b; Ishida 2013) and DUNE (Abi et al. 2020). The excess of electron neutrino flux reported by the SBL experiments LSND (Aguilar-Arevalo et al. 2001) and MiniBooNE (Aguilar-Arevalo et al. 2018) may hint at the existence of new physics. Currently, these anomalies are being studied by experiments like JSNS^2 (Ajimura et al. 2021) and MicroBooNE (Abratenko et al. 2022).

Depending on the neutrino energy E and the distance L between the source and the detector, neutrino oscillation experiments are sensitive to different values of the mass splitting $|\Delta m^2|$. In Table 1, we summarize the characteristic values for different types of neutrino experiments and the corresponding mass splitting to which these experiments are most sensitive to flavor oscillations in vacuum.

Combining all the available neutrino oscillation results from different experiments allows to better constrain the neutrino mass and mixing parameters. This has been done in the last few years by several independent groups through global fits to neutrino data (Capozzi et al. 2021; de Salas et al. 2021; Esteban et al. 2020). In Table 2 we summarize the most recent results for θ_{12}, θ_{23}, θ_{13}, Δm^2_{21}, $|\Delta m^2_{31}|$ and δ obtained in the global analysis performed by (de Salas et al. 2021), for normal ordering (NO) of the neutrino mass spectrum, i.e. $m_1 < m_2 < m_3$, and inverted ordering (IO) with $m_3 < m_1 < m_2$.

Looking at the current data, we conclude that the three mixing angles, the solar mass splitting and the absolute

TABLE 1 Characteristic values of the neutrino energy E and the distance L between the source and the detector, for different neutrino experiments. The mass splitting $|\Delta m^2|$ at which these experiments are most sensitive is also given.

Experiment	E (MeV)	L (m)	$\lvert\Delta m^2\rvert$ (eV^2)
Solar	1	10^{10}	10^{-10}
Atmospheric	$10^2 - 10^5$	$10^3 - 10^7$	$10^{-4} - 10^{-1}$
Reactor (SBL)	1	$10^2 - 10^3$	$10^{-3} - 10^{-2}$
Reactor (LBL)	1	$10^4 - 10^5$	$10^{-5} - 10^{-4}$
Accelerator (SBL)	$10^3 - 10^4$	10^2	$> 10^{-1}$
Accelerator (LBL)	$10^3 - 10^4$	$10^5 - 10^6$	$10^{-3} - 10^{-2}$

TABLE 2 Allowed ranges for the mixing angles, the Dirac CP phase, and neutrino mass-squared differences, obtained from a global fit of neutrino oscillation data (de Salas et al. 2021).

Parameter	Best Fit $\pm 1\sigma$	3σ range
$\theta_{12}(^\circ)$	34.3 ± 1.0	$31.4 \to 37.4$
$\theta_{23}(^\circ)$ [NO]	49.26 ± 0.79	$41.20 \to 51.33$
$\theta_{23}(^\circ)$ [IO]	$49.46^{+0.60}_{-0.97}$	$41.16 \to 51.25$
$\theta_{13}(^\circ)$ [NO]	$8.53^{+0.13}_{-0.12}$	$8.13 \to 8.92$
$\theta_{13}(^\circ)$ [IO]	$8.58^{+0.12}_{-0.14}$	$8.17 \to 8.96$
$\delta(^\circ)$ [NO]	194^{+24}_{-22}	$128 \to 359$
$\delta(^\circ)$ [IO]	284^{+26}_{-28}	$200 \to 353$
Δm^2_{21} ($\times 10^{-5}$ eV^2)	$7.50^{+0.22}_{-0.20}$	$6.94 \to 8.14$
$\lvert\Delta m^2_{31}\rvert$ ($\times 10^{-3}$ eV^2) [NO]	$2.55^{+0.02}_{-0.03}$	$2.47 \to 2.63$
$\lvert\Delta m^2_{31}\rvert$ ($\times 10^{-3}$ eV^2) [IO]	$2.45^{+0.02}_{-0.03}$	$2.37 \to 2.53$

value of the atmospheric mass splitting are well determined. On the other hand, the sign of Δm^2_{31} (and thus the mass ordering of neutrinos), the octant of the mixing angle θ_{23} (which is close to $\pi/4$), and also the CP phase δ need to be confirmed yet. In particular, tests for leptonic CP violation would be accessible in long-baseline and atmospheric neutrino experiments, by measuring the difference in the oscillation probabilities $P(\nu_\mu \to \nu_e)$ and $P(\overline{\nu}_\mu \to \overline{\nu}_e)$. Presently, although for an IO mass spectrum the determination of δ in different accelerator experiments leads to compatible values (close to maximal CP violation), a tension remains between the preferred values of δ reported by T2K (Abi et al. 2020; Dunne 2020) and NOνA (Acero et al. 2019; Himmel 2020) experiments for a NO spectrum. Clearly, the current preference for a nonzero CP phase may signal the existence of leptonic CP violation in nature. For a comprehensive review on this topic, we refer the reader to Branco et al. (2012).

The above open questions will be certainly targeted by next-generation neutrino experiments and, in turn, new global fits of neutrino oscillation data would be able to determine the still unknown oscillation parameters.

2.2 | Absolute neutrino mass scale

Since flavor oscillations are not sensitive to the absolute neutrino mass scale, other laboratory and cosmological probes are used to get information on this quantity. In particular, a model-independent information on the absolute neutrino mass scale can be obtained from the kinematics of weak decays involving neutrinos (Formaggio et al. 2021), namely from the measurement of the endpoint of the electron energy spectrum in β-decays. The relevant observable is the effective electron neutrino mass given by

$$m_\beta = \sqrt{\sum_i |U_{ei}|^2 m_i^2}, \tag{6}$$

in the standard 3ν mixing framework.

Upper bounds on the effective electron neutrino mass can be extracted from β emission in tritium. Presently, the most stringent bound is given by KATRIN experiment, $m_\beta < 0.8$ eV at 90% CL (Aker et al. 2022), which is expected in near future to be sensitive to an effective mass as low as 0.2 eV at 90% CL (Aker et al. 2021). The Project 8 collaboration (Asner et al. 2015) expects to achieve a sensitivity limit of $m_\beta \sim 40$ meV, using cyclotron radiation emission spectroscopy, thus covering the IO mass region. Other current experiments such as ECHo (Gastaldo et al. 2017) and HOLMES (Giachero et al. 2017) expect to reach the limit $m_\beta \sim 1-2$ eV, using electron capture in holmium-163.

Another constraint on the neutrino mass scale can be obtained from lepton number violating neutrinoless double beta ($0\nu\beta\beta$) decay. This is a rare nuclear decay process, where two neutrons are converted into two protons with the emission of two electrons, as in the process $N(Z,A) \to N(Z+2,A) + 2e^-$, where $N(Z,A)$ is a nucleus with atomic number Z and mass number A. The simplest process allowing for $0\nu\beta\beta$ decay occurs with the exchange of a virtual Majorana light neutrino, assuming only the SM fields. In this case, the decay rate is simply given by $\Gamma_{0\nu\beta\beta}(N) = G_N |\mathcal{M}_N|^2 \, m^2_{\beta\beta}$ (Dolinski et al. 2019), where G_N is the phase space factor and $\mathcal{M}_N$ is the nuclear matrix element of the nucleus. The parameter $m_{\beta\beta}$, also called the effective electron neutrino Majorana mass, depends on the neutrino masses and the PMNS mixing parameters as

$$m_{\beta\beta} = \left| \sum_i U^2_{ei} m_i \right|. \tag{7}$$

The strongest bound on the $0\nu\beta\beta$ decay comes from the liquid scintillator experiment KamLAND-Zen 800 (Abe et al. 2023), which leads to an upper bound for $m_{\beta\beta}$ in the range $36-156$ meV and partially probes the IO mass region. Combining neutrino oscillation data with KamLAND-Zen results already excludes degenerate neutrinos with a lightest mass larger than 0.7 eV. Similar constraints come from other experiments, such as the upper bounds $93-286$ meV from EXO-200 (Anton et al. 2019), $79-180$ meV from GERDA (Agostini et al. 2020), and $90-305$ meV from CUORE (Adams et al. 2022). Future experiments like JUNO (Zhao et al. 2017), LEGEND-1000 (Abgrall et al. 2017), nEXO (Albert et al. 2018), NEXT-HD (Gomez-Cadenas 2019), KamLAND2-Zen (Nakamura et al. 2020) AMORE-II (Lee 2020), SNO+ Phase II (Albanese et al. 2021), and CUPID-1T (Armatol et al. 2022) are expected to reach $m_{\beta\beta}$ in the range of $5-20$ meV, thus probing partially the NO parameter space and completely the IO mass region.

Constraints on the mass scale of neutrinos obtained from astrophysical and cosmological data are competitive with those obtained in laboratory experiments. Indeed, from oscillation experiments, we know that at least two neutrino have nonzero masses. If one assumes the standard thermal evolution of the Universe, the contribution of neutrinos to the total energy density is given by Workman et al. (2022)

$$\Omega_\nu = h^{-2} \left(\frac{\sum_i m_i}{93.14 \text{ eV}} \right), \tag{8}$$

where $h \simeq 0.67$ is the scaling factor for Hubble expansion rate.

The tightest bound on the sum of neutrino masses $\sum_i m_i$ comes from current cosmological observations, using Planck satellite data for CMB anisotropies in

temperature and polarization, combined with different astrophysical datasets (Aghanim et al. 2020). Assuming the based-ΛCDM model, Planck leads to the upper bounds $\sum_i m_i < 0.54$ eV (considering only TT+lowE data) and $\sum_i m_i < 0.26$ eV (considering TT,TE,EE+lowE data) at 95% CL (Aghanim et al. 2020). If the above constraints are combined with baryon acoustic oscillation (BAO) data, the bound tightens further, yielding $\sum_i m_i < 0.12$ eV, which already puts pressure on the IO mass hierarchy. Upcoming and next-generation CMB surveys combined with large-scale structure measurements are expected to measure the sum of neutrino masses at a 1σ sensitivity level of 15 meV (Lattanzi et al. 2020).

In Figures 1–3, we present the currently allowed regions for m_β, $m_{\beta\beta}$, and $\sum_i m_i$, respectively, as functions of the lightest neutrino mass $m_0 = m_1\,(m_3)$, for NO (IO) neutrino mass spectrum. The results are obtained by varying the neutrino observables given in Table 2 in their 3σ range. The horizontal dashed lines in Figure 1 correspond to the current (in green) and expected (in orange) upper bounds at 90% CL in KATRIN experiment, while the magenta line indicates the expected sensitivity of Project 8 collaboration—Phase IV. In Figure 2, the magenta region corresponds to the upper-bound range imposed by the KamLAND-Zen 800 experiment. Finally, the horizontal dashed lines in Figure 3 correspond to the cosmological upper bounds reported by Planck Collaboration considering TT+lowE data (green line), TT,TE,EE+lowE data (orange line), and TT,TE,EE+lowE+BAO data (magenta line) at 95% CL.

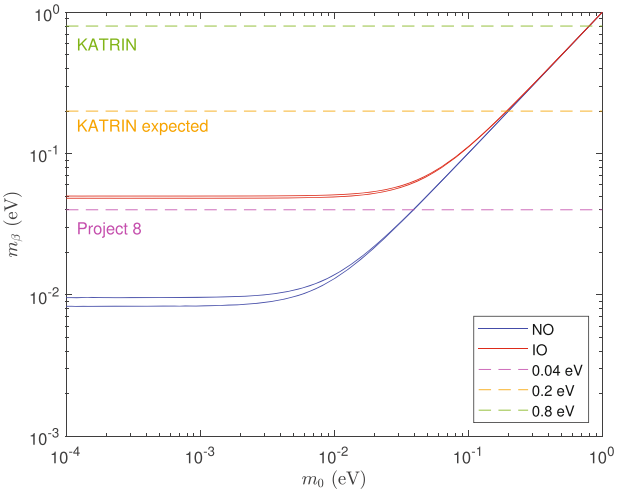

FIGURE 1 The effective mass m_β as a function of the lightest neutrino mass $m_0 = m_1\,(m_3)$ for NO (IO), taking into account the 3σ range of the neutrino observables given in Table 2. The horizontal dashed lines correspond to the current (in green) and expected (in orange) upper bounds at 90% CL in KATRIN experiment, while the magenta line indicates the expected sensitivity of Project 8 collaboration—Phase IV.

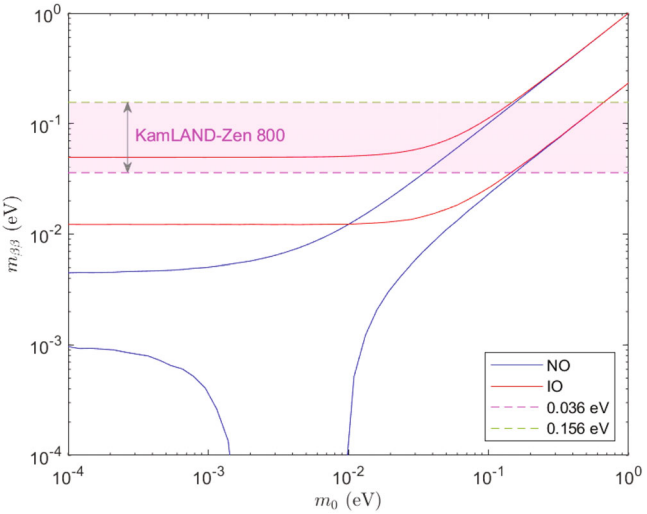

FIGURE 2 The effective Majorana mass $m_{\beta\beta}$ as a function of the lightest neutrino mass $m_0 = m_1\,(m_3)$ for NO (IO), taking into account the 3σ range of the neutrino observables given in Table 2. The magenta region corresponds to the upper-bound range imposed by the KamLAND-Zen 800 experiment.

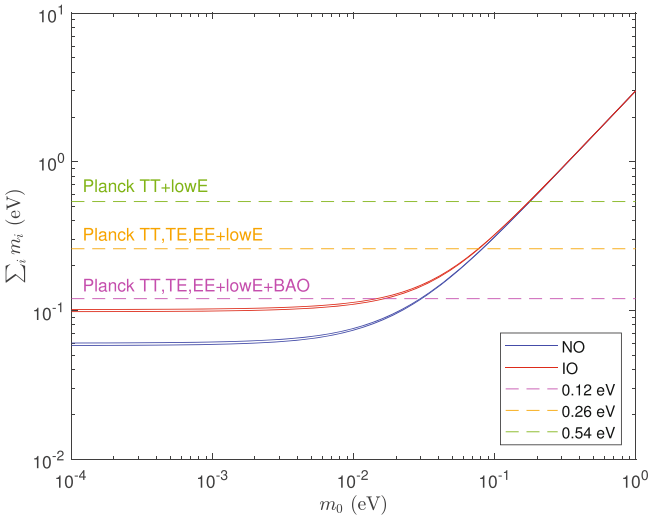

FIGURE 3 Sum of the neutrino masses as a function of the lightest mass $m_0 = m_1\,(m_3)$ for NO (IO), taking into account the 3σ range of the neutrino observables given in Table 2. The horizontal dashed lines correspond to the cosmological upper bounds reported by Planck Collaboration, considering TT+lowE data (in green), TT,TE,EE+lowE (in orange), and TT,TE,EE+lowE+BAO data (in magenta) at 95% CL.

Massive stars, like supernova, are an important source of neutrinos, and it is possible to get information about the absolute neutrino mass scale from the detection of neutrino bursts from the core collapse of such stars. This is so because neutrino propagation from a supernova to a neutrino detector will result in an energy-dependent time delay with respect to propagation at the speed of light given by $\Delta t\ [\mathrm{s}] = 0.515\ D[\mathrm{kpc}] \times (m_\nu[\mathrm{eV}]/E_\nu[\mathrm{MeV}])^2$,

where D is the distance to the star (Sajjad Athar et al. 2022). Although the detectable range for current neutrino detectors is approximately $D \sim$ tens of kpc (Milky Way), next-generation detectors such as Hyper-Kamiokande (Abe et al. 2018b) are expected to reach neutrino events at $D \sim 700$ kpc. At present, the strongest bound coming from these sources is $m_\nu < 6$ eV (Loredo & Lamb 2002; Pagliaroli et al. 2010), obtained from a time delay $\Delta t = 13$ s of the observed $\overline{\nu}_e$ burst from SN1987A at $D = 55$ kpc. Unfortunately, these bounds are not yet competitive with the limits set by KATRIN experiment.

2.3 | Beyond the 3ν picture

Despite the success of the 3ν scenario in explaining oscillation data, there are a few experimental hints pointing toward the existence of eV-mass sterile neutrinos, which do not couple to SM weak interactions.[3] In particular, anomalies at $E/L \sim \Delta m^2 \sim 1$ eV^2 have been observed in SBL accelerator and reactor neutrino experiments. Let us briefly comment on them.

The LSND experiment (Aguilar-Arevalo et al. 2001) reported a signal in the oscillation channel $\overline{\nu}_\mu \to \overline{\nu}_e$, corresponding to a large mass splitting that cannot be accommodated within the framework of three active neutrinos. The MiniBooNE experiment (Aguilar-Arevalo et al. 2018) has also reported an event excess in the low-energy region of the electron neutrino and anti-neutrino spectra at a similar $L/E \sim 1$ eV^2 ratio. This signal could be explained if the existence of a sterile neutrino is assumed. Several new experiments are expected to check the sterile neutrino hypothesis, for example, the accelerator based experiment JSNS^2 (Ajimura et al. 2021) at J-PARC.

The so-called *Gallium anomaly* has been reported in radioactive source experiments at the Gallium solar neutrino experiments (Barinov et al. 2022; Kaether et al. 2010). In this case, an event rate of ν_e lower than expected has been observed, which could be explained with a sterile neutrino, assuming that the ν_e disappearance is due to oscillations with $\Delta m^2 \sim 1$ eV^2. There is also the so-called *reactor antineutrino anomaly*, which theoretically predicts a neutrino rate (of the $\overline{\nu}_e$ flux emitted by nuclear reactors) higher than observed in the SBL reactor experiments (Giunti et al. 2022; Mueller et al. 2011). Such an anomaly could be interpreted as the disappearance of reactor antineutrinos due to flavor oscillations with a mass splitting ~ 1 eV^2 (Mention et al. 2011).

[3]While there is presently no constraint on the number of sterile neutrino states (Dasgupta & Kopp 2021), LEP collider measurements of the invisible decay width of the Z boson imply the existence of only three light active neutrinos.

It is worth emphasizing that although the above anomalies may find an explanation postulating a sterile neutrino, there exists currently a tension between appearance and disappearance oscillation experiments, since so far the latter have not observed any signal in the same parameter space. Furthermore, additional constraints on light sterile neutrino scenarios are imposed by cosmological observations, considering the bounds on the sum of neutrino masses and the effective number of relativistic neutrino states in thermal equilibrium in the early Universe (Aghanim et al. 2020). From the combined analysis of Planck data at 95% CL, it follows that a light sterile neutrino is allowed provided that $N_{\rm eff} < 3.34$ and the effective mass of the sterile neutrino $m_{\rm eff} = \Omega_\nu h^2\ (94.1\ {\rm eV}) < 0.23$ eV.

Finally, there may also exist sterile neutrinos with a mass scale much above the eV-range. Particularly interesting is the keV-mass region, since keV sterile neutrinos may become warm dark matter candidates (Abazajian 2017; Boyarsky et al. 2019; Drewes et al. 2017) or be even connected with the generation of pulsar kicks (Fuller et al. 2003; Kusenko & Segre 1997). The existence of much heavier sterile neutrinos could be motivated, for instance, in connection with the seesaw mechanism for the generation of the light neutrino masses and the leptogenesis mechanism for the explanation of the matter–antimatter asymmetry observed in the Universe. For a more detailed discussion on the properties of sterile neutrinos we refer the reader to the recent reviews on the status and perspectives in neutrino physics (Sajjad Athar et al. 2022) and on the synergy between cosmological and laboratory searches (Gerbino et al. 2022).

Going beyond the 3ν framework, one can also envisage new neutrino interactions besides the weak interactions. These new interactions are typically parameterized by effective four-fermion operators, involving additional vector-like interactions of the left-handed SM neutrinos with other fermions, and whose strength is characterized by dimensionless complex parameters encoding deviations from standard interactions. In fact, many models for neutrino masses predict the existence of neutral-current and charged-current nonstandard neutrino interactions (NSI). The latter not only can impact the coherent scattering of neutrinos in matter, but also lead to the breaking of the lepton flavor universality and to flavor-changing neutral-current processes.

Since neutrino oscillation experiments are sensitive to NSI, these interactions may influence global analyses of oscillation data. One of the neutrino oscillation parameters affected in the presence of NSI is the solar mixing angle θ_{12}. In this case, besides the standard solution $\theta_{12} < \pi/4$ obtained in the 3ν picture, a new solution with $\theta_{12} > \pi/4$ is also allowed (Miranda et al. 2006). This is due to the fact

that there exist intrinsic degeneracies in the NSI-induced matter Hamiltonian describing neutrino oscillations. A more detailed discussion on NSI can be found in (Berryman et al. 2022; Farzan & Tortola 2018).

3 | THEORETICAL CHALLENGES

3.1 | Are neutrinos Dirac or Majorana particles?

If neutrinos and antineutrinos were different particles, described by two different fields, then they would be Dirac-type particles, similar to quarks and charge leptons. On the other hand, if a neutrino is its own antiparticle, we say that it is a Majorana-type particle, being both states described by a single field. In the latter case, the left and right chiral components of the Majorana field are not independent, $\nu_R \equiv \nu_L^c = C\overline{\nu}^T$, where $C = i\gamma^2\gamma^0$ is the charge conjugation matrix. Since for a Majorana neutrino $\nu = \nu_L + \nu_R = \nu^c$, the neutrino field can be represented by a two-component spinor, unlike a Dirac fermion that is described by a four-component spinor.

The fact that neutrinos can have either Dirac or Majorana nature has important consequences for neutrino mass models, as we shall see shortly. From the experimental point of view, unveiling the neutrino nature remains a challenge, since all observables that can distinguish neutrinos of a given nature are highly suppressed by powers of the tiny neutrino masses. Presently, the most promising path is the observation (or not) of neutrinoless double beta decay. An observation of this decay will provide a convincing evidence for the existence of Majorana neutrinos. Yet, the nonobservation of $0\nu\beta\beta$ decay does not guarantee the existence of Dirac neutrinos, unless a definite signal in neutrinoless quadruple beta decay is simultaneously observed (Hirsch et al. 2018).

In the SM, the three active neutrinos $\nu_{\alpha L}$ ($\alpha = e, \mu, \tau$) reside in $SU(2)_L$ lepton doublets. Independently of their nature, neutrinos interact with the charged leptons ℓ_α through the charged-current (CC) interaction Lagrangian

$$-\mathcal{L}_{\rm CC} = \frac{g}{\sqrt{2}} \sum_\alpha \overline{\nu_{\alpha L}}\, \gamma^\mu \ell_\alpha^- W_\mu^+ + \text{h.c.} \qquad (9)$$

Similarly, neutrinos can interact among themselves through the neutral-current (NC) interaction Lagrangian

$$-\mathcal{L}_{\rm NC} = \frac{g}{2\cos\theta_W} \sum_\alpha \overline{\nu_{\alpha L}}\, \gamma^\mu \nu_{\alpha L} Z_\mu^0 + \text{h.c.}, \qquad (10)$$

where g is the $SU(2)$ gauge coupling constant and θ_W is the Weinberg angle. Thus, neutrinos can be produced in the decays of the $W^\pm$ and Z gauge bosons.

The interactions given in Equations (9) and (10) conserve the total lepton number $L = L_e + L_\mu + L_\tau$, where L_α denote the individual lepton family numbers. We recall that the SM Lagrangian is invariant at tree level under the accidental global symmetry $U(1)_B \times U(1)_e \times U(1)_\mu \times U(1)_\tau$, which implies the conservation of the baryon number B and each lepton flavor number. The discovery of neutrino oscillations leads irrefutably to L_α violation.[4] If $0\nu\beta\beta$ decay is observed, the violation of the total lepton number L would be also established. At nonperturbative level, the $B - L$ symmetry remains accidentally conserved, while $B + L$ is violated by weak instantons, although with a highly suppressed rate $\Gamma_{B+L}^{\rm inst} \simeq e^{-16\pi^2/g^2} \sim 10^{-173}$ ('t Hooft, G. 1976). Remarkably, in early Universe, at temperatures above the electroweak phase transition $T_{\rm ew} \sim 100$ GeV, such nonperturbative configurations, usually called sphalerons, turn out to be unsuppressed, with an interaction rate $\Gamma_{B+L}^{\rm sph} \propto T$. As temperature drops below $T_{\rm ew}$, the sphaleron rate becomes Boltzmann suppressed, $\Gamma_{B+L}^{\rm sph} \propto e^{-E_{\rm sph}/T}$, where $E_{\rm sph}$ is the sphaleron energy. Such a distinctive feature suggests that sphaleron transitions may have played a crucial role in generating the matter–antimatter asymmetry observed in the Universe (Kuzmin et al. 1985).

3.2 | How are neutrino masses generated?

In the SM, fermion masses arise from the Dirac-type Yukawa interactions $Y_f \overline{\psi_L} \phi\, \psi_R$ between the fermion states ψ and the Higgs field ϕ, where the chiral left-handed (right-handed) states transform as doublets (singlets) of the gauge group $SU(2)_L$. Once the neutral component of the Higgs field acquires a nonzero vacuum expectation value $v \simeq 246$ GeV, the $SU(2)_L$ symmetry is spontaneously broken (Higgs mechanism) and all SM fermions acquire masses $m_f = Y_f v/\sqrt{2}$. Since the particle content of the SM does not include right-handed (RH) neutrino fields, neutrinos are strictly massless in this model. Thus, new physics beyond the SM is necessary to explain neutrino masses.

Assuming that neutrinos are Dirac particles and lepton number is conserved, one can generate their masses in analogy to other SM charged fermions by simply introducing new sterile states ν_R, singlets under the SM gauge group, that couple to the Higgs field and charged leptons through the Yukawa interaction term $Y_\nu \overline{\ell_L} \tilde{\phi}\, \nu_R$, where $\tilde{\phi} \equiv i\tau^2\phi^*$. After the electroweak symmetry breaking

[4] Flavor violation has not been observed for charged leptons, being the tightest bounds set by the decays $\mu \to e\gamma$ (Baldini et al. 2016) and $\mu \to 3e$ (Bellgardt et al. 1988).

(EWSB), neutrino masses will be simply given by $m_\nu = Y_\nu v/\sqrt{2}$. Since neutrino oscillation data imply $m_\nu \sim \mathcal{O}(0.1)$ eV, Yukawa couplings of the order of 10^{-13} would be required to reproduce the light neutrino masses. We recall that the smallest charged-lepton Yukawa coupling is that of the electron, $Y_e \simeq 10^{-5}$, which resides in the same $SU(2)_L$ doublet as ν_e. Thus, Y_ν should be at least 8 orders of magnitude smaller than Y_e, a hierarchy that would be arguably unnatural from the theoretical viewpoint. A naturally small Dirac neutrino mass can be obtained, for instance, if the symmetry of the SM is enlarged in such a way that the dimension-four Yukawa term is forbidden and an effective m_ν, suppressed by a large mass scale, is constructed at tree level or at one loop (Ma & Popov 2017).

Considering the SM as an effective low-energy theory at the electroweak scale, Majorana neutrino masses can be generated through the unique dimension-five operator, the so-called Weinberg operator (Weinberg 1979), that violates lepton number by two units ($\Delta L = 2$):

$$\mathcal{L}_{d=5} \sim \frac{1}{M}\left(\overline{\ell_L^c}\tilde{\phi}^*\right)\left(\tilde{\phi}^\dagger \ell_L\right) + \text{h.c.}, \tag{11}$$

where M is the scale of new physics. After the EWSB, Majorana masses $\sim v^2/M$ are obtained, which are suppressed by the high-energy scale M. For $M \sim 10^{14}$ GeV, sub-eV neutrino masses can then be generated.

One may wonder about the possible ultraviolet completions of the Weinberg operator in a renormalizable gauge theory (Bonnet et al. 2012). Perhaps the most popular and attractive realization is through the so-called seesaw mechanism (see, e.g., refs. Mohapatra et al. 2007 and Nunokawa et al. 2008), in which the operator is induced by the exchange of heavy particles with a mass scale $M \gg v$. Depending on the $SU(2)_L$ contraction of the ℓ_L and ϕ doublets in the Weinberg operator, the mediators can be a singlet fermion ν_R, a triplet scalar Δ, or a triplet fermion Σ, leading respectively to three realizations of the seesaw mechanism at tree level: type-I seesaw (Gell-Mann et al. 1979; Glashow 1980; Minkowski 1977; Mohapatra & Senjanovic 1980; Schechter & Valle 1980; Yanagida 1979), type-II seesaw (Cheng & Li 1980; Konetschny & Kummer 1977; Lazarides et al. 1981; Mohapatra & Senjanovic 1981; Schechter & Valle 1980), and, finally, the type-III seesaw (Foot et al. 1989).

For illustration, let us consider the type-I seesaw mechanism, which is schematically represented in the left diagram of Figure 4. In this case, after EWSB, the mass terms in the Lagrangian can be written in compact form

$$-\mathcal{L}_{\text{mass}} = \frac{1}{2}\overline{n_L^c}\mathcal{M}\, n_L + \text{h.c.}, \quad \mathcal{M} = \begin{pmatrix} 0 & m_D \\ m_D^T & M_R \end{pmatrix}, \tag{12}$$

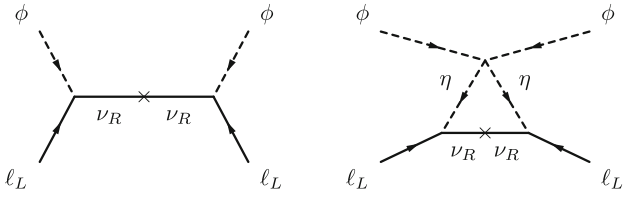

FIGURE 4 Examples of mechanisms for the generation of Majorana neutrino masses. Left diagram: Type-I seesaw mechanism mediated by singlet fermions ν_R. Right diagram: Scotogenic mechanism mediated by singlet fermions ν_R and an inert scalar doublet η.

where $n_L = (\nu_L\ \nu_R^c)^T$, m_D is the Dirac neutrino mass matrix, and M_R corresponds to the Majorana bare mass term. The latter is not protected by the SM gauge symmetries and thus can be arbitrarily large. Note also that due to gauge invariance a Majorana term cannot be written for the $SU(2)_L$ doublet ν_L. After diagonalising the full mass matrix, the light neutrino masses are given by

$$m_\nu \simeq -m_D M_R^{-1} m_D^T. \tag{13}$$

So, the heavier M_R the lighter m_ν. Clearly, to reproduce the observed neutrino masses, very large values of M_R are required, which are outside the reach of current colliders.

Low-scale seesaw variants with testable phenomenology can also be constructed. For instance, the so-called inverse seesaw model (Mohapatra 1986; Mohapatra & Valle 1986), in which two $SU(2)_L$ singlet Majorana fermions, ν_R and S, are introduced, yields a Lagrangian similar to (12), with $n_L = (\nu_L\ \nu_R^c\ S)^T$ and a mass matrix given by

$$\mathcal{M} = \begin{pmatrix} 0 & m_D & 0 \\ m_D^T & 0 & M_R \\ 0 & M_R^T & m_S \end{pmatrix}. \tag{14}$$

This leads to the light neutrino mass matrix

$$m_\nu \simeq -m_D (M_R m_S^{-1} M_R^T)^{-1} m_D^T. \tag{15}$$

In this double-seesaw formula, neutrino mass suppression is guaranteed by small lepton number violating mass parameters. Since in the limit $m_S \to 0$ lepton number is conserved, the inverse seesaw provides a natural framework in the 't Hooft sense ('t Hooft, G. 1980). A remarkable feature of this mechanism is that small Majorana neutrino masses can be generated with RH neutrino masses at the TeV scale (or below) and unsuppressed (order-one) Yukawa couplings, and thus these models could be testable at colliders.

Mechanisms that generate neutrino masses at loop level are also conceivable. Examples at one-loop order are the Zee model (Zee 1980) and the scotogenic model (Ma 2006). An implementation of the canonical scotogenic mechanism is depicted in the right diagram of Figure 4, in which singlet fermions ν_R and an inert scalar doublet η mediate neutrino mass, which is generated through a Majorana mass term for ν_R and a quartic coupling between the Higgs field ϕ and the scalar doublet η. Assuming that these fields have an odd charge under a Z_2 symmetry, a tree-level mass term is forbidden. An important feature of this model is that either the lightest of the new fermions or the lightest of the dark neutral scalars can be a dark matter candidate, stabilized by the Z_2 symmetry.

In summary, several mechanisms for the generation of neutrino masses are viable, which are distinguishable by their particle content, couplings of the new particles to the SM fields, and energy scales for new physics. Confronting these models with experiments will be of utmost importance to ultimately understand the origin of the tiny neutrino masses.

3.3 | Are neutrinos responsible for the cosmic matter-antimatter asymmetry?

No primordial antimatter is found in our observable Universe. The imbalance between matter and antimatter can be quantified in terms of the baryon-to-photon ratio $\eta_B = (n_B - n_{\overline{B}})/n_\gamma$, where $n_B, n_{\overline{B}}$, and n_γ are the number densities of baryons, antibaryons, and photons, respectively. The combined analysis of Planck TT, TE, EE + lowE + lensing data yields the value $\eta_B = (6.12 \pm 0.04) \times 10^{-10}$ (Aghanim et al. 2020), which is also consistent with the limits imposed by the concordance of the light elements and big bang nucleosynthesis. Since any primordial asymmetry would have been exponentially washed out during the inflationary period, the amount of baryon asymmetry must be dynamically generated after inflation. The necessary ingredients for a successful implementation of a dynamical mechanism are well known (Sakharov 1967): B-violation, C and CP violation, and departure from thermal equilibrium.

Among the viable scenarios to explain the cosmic matter–antimatter asymmetry, leptogenesis is an attractive and well-motivated mechanism (Fukugita & Yanagida 1986). In its simplest realization, new heavy particles are introduced in the theory in such a way that the interactions relevant for leptogenesis are simultaneously responsible for the seesaw neutrino masses. The three Sakharov conditions are naturally fulfilled in this framework. Indeed, the seesaw mechanism requires lepton number violation and nonperturbative $(B + L)$-violating sphaleron processes will partially convert the lepton asymmetry into a baryon asymmetry; CP can be explicitly violated by complex Yukawa couplings[5]; finally, the departure from thermal equilibrium is accomplished by the out-of-equilibrium decays of the new heavy particles at temperatures above the electroweak scale.

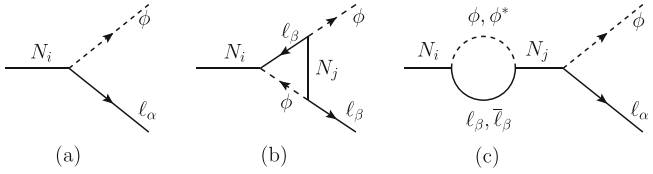

FIGURE 5 Feynman diagrams contributing to the CP asymmetries ϵ_i^α in type-I seesaw leptogenesis: (a) Tree-level graph, (b) one-loop vertex graph, and (c) one-loop self-energy graphs.

Let us consider, for instance, the simple SM extension with RH neutrinos, in the context of the type-I seesaw model. The relevant interactions are described by the Dirac Yukawa couplings Y_ν that couple the Higgs field ϕ and the charged leptons ℓ with the RH neutrinos ν_R. Working in the mass eigenbasis of the charged leptons ℓ_α $(\alpha = e, \mu, \tau)$, and in the mass eigenbasis N_i of the neutrinos ν_{Ri}, the CP asymmetry ϵ_i^α in the lepton flavor α produced in the N_i decays is defined as

$$\epsilon_i^\alpha \equiv \frac{\Gamma(N_i \to \phi\, \ell_\alpha) - \Gamma(N_i \to \phi^\dagger\, \overline{\ell_\alpha})}{\sum_\beta \left[\Gamma(N_i \to \phi\, \ell_\beta) + \Gamma(N_i \to \phi^\dagger\, \overline{\ell_\beta})\right]}, \tag{16}$$

where $\Gamma(\cdots)$ denotes the decay rate of the corresponding channel. A nonvanishing CP asymmetry ϵ_i^α is then obtained from the interference of the tree-level and one-loop diagrams depicted in Figure 5. Summing over the lepton flavors, the total unflavored asymmetry $\epsilon_i = \sum_\alpha \epsilon_i^\alpha$ is obtained.

Assuming that the Universe reheats to a thermal bath after inflation, the final baryon-to-photon number ratio η_B can be estimated as the product of three suppression factors: (the CP asymmetry ϵ_i in N_i-decays) × (an efficiency factor κ_i, which is estimated by solving the relevant Boltzmann equations and accounts for the washout effects in decays, inverse decays, and scattering processes) × (a reduction factor due to chemical equilibrium, charge conservation, and the redistribution of the asymmetry among different particle species). This is the so-called thermal leptogenesis mechanism and has been successfully implemented in several neutrino models and

[5]CP can also be spontaneously broken by a complex vacuum expectation value of a scalar field, generating complex physical phases in the lepton sector.

extensively studied in the literature (see, e.g., Buchmuller et al. 2005a,b; Davidson et al. 2008).[6]

In the case of very hierarchical RH neutrinos, leptogenesis requires the mass of the lightest neutrino N_1 to be quite large, $M_1 \gtrsim 10^9$ GeV. Nevertheless, leptogenesis may not necessarily occur at high energies. Indeed, assuming quasi-degenerate heavy neutrino masses, leptogenesis could take place resonantly and much lower values of M_1 be allowed (Pilaftsis & Underwood 2004). Quasi-degenerate masses naturally appear, for instance, in the so-called radiative leptogenesis scenarios, where the mass splitting is completely induced by renormalization group effects (González Felipe et al. 2004; Turzynski 2004). An attractive feature of low-scale leptogenesis is that it can be tested in laboratory experiments (Agrawal et al. 2021; Alekhin et al. 2016; Chun et al. 2018).

As a final comment we note that, if neutrinos are Dirac particles, baryogenesis may proceed via the Dirac leptogenesis mechanism (Dick et al. 2000), since neutrino Yukawa couplings are small enough to hide their RH lepton number from sphalerons during the electroweak epoch.

3.4 | Occam's razor vs. symmetry principle

In the spirit of Occam's razor principle, which states that *plurality is not to be assumed without necessity*, it is desirable to construct physical models that contain the minimal number of free parameters, making the least number of assumptions. In the context of a neutrino mass model where light neutrino masses arise from the type-I seesaw mechanism, introducing only two RH neutrinos would be sufficient. This is so because current neutrino oscillation data do not preclude the existence of a massless neutrino. Remarkably, the same two RH neutrinos are enough for implementing the thermal leptogenesis mechanism in this model. Thus, Occam's razor principle would urge us to consider just a simple extension of the SM with two RH neutrinos (2RHNSM).

Regarding the total number of free parameters in the minimal scenario described above, the Lagrangian of the neutrino sector contains 11 parameters at high energies: 2 heavy Majorana masses and 9 real parameters (six moduli and three phases) needed to specify the 3×2 Yukawa coupling matrix Y_ν. Since the two Majorana masses can be absorbed into Y_ν by an appropriate rescaling of its elements, only nine parameters are independent as far as the light neutrino seesaw mass matrix is concerned. On the other hand, there are seven quantities associated to the latter matrix, measurable at low energies: two light neutrino masses, three mixing angles, one Dirac CP phase and one Majorana phase. Therefore, there remain two free parameters in this model. Notice also that, since one neutrino is massless, the remaining two neutrino masses are fixed by the squared-mass differences Δm^2_{21} and Δm^2_{31}, already measured in oscillation experiments. Thus, the absolute neutrino mass scale is predicted in the 2RHNSM. Furthermore, a clear dependence of the effective Majorana mass parameter $m_{\beta\beta}$ on the physical Majorana phase α is observed, for both NO and IO spectra, as shown in Figure 6.

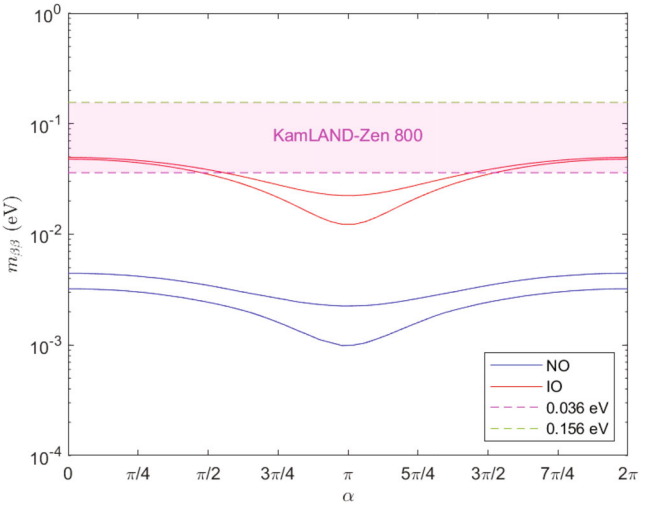

FIGURE 6 The $m_{\beta\beta}$ parameter in the 2RHNSM, as a function of the Majorana phase α, taking into account the 3σ range of neutrino observables. The magenta region corresponds to the upper-bound range of the KamLAND-Zen 800 experiment.

In order to further reduce the number of free parameters at high energies and get predictability, we could invoke again Occam's razor principle in the 2RHNSM (Harigaya et al. 2012). One of the simplest possibilities is to assume that, in a given weak basis, there exist vanishing matrix elements (*texture zeros*) in the Yukawa coupling and/or mass matrices of the lepton sector. For instance, in the charged-lepton mass basis, the imposition of two texture zeros in the Dirac Yukawa coupling Y_ν of the 2RHNSM was first motivated by the possibility of relating the sign of the baryon asymmetry of the Universe to CP violation in neutrino oscillation experiments (Frampton et al. 2002). It was later shown that, while for an IO of neutrino masses such textures are still phenomenologically viable, for a NO spectrum they are excluded by recent oscillation data (Barreiros et al. 2018; Harigaya et al. 2012).

Several systematic studies of textures zeros in the leptonic sector can be found in the literature; see, for instance, refs. Borgohain & Borah (2021), Cebola et al. (2015), Ludl & Grimus (2014). In any search for experimentally viable

[6] Leptogenesis may also take place nonthermally, with the heavy particles generated by inflaton decays (Asaka et al. 1999) or during the preheating period (Giudice et al. 1999).

texture-zero structures for fermion mass matrices, it is important to take into account the freedom to make weak basis transformations, which do not change the physical content. In particular, if some zeros can be obtained starting from arbitrary mass matrices, by making appropriate weak basis transformations that leave the gauge currents flavor diagonal, they have no physical meaning by themselves (Branco et al. 2009; Emmanuel-Costa & González Felipe 2017).

In a different perspective, symmetries can be introduced in neutrino mass models with the aim of explaining the appearance of zeros in some elements of the mass matrices. It is well known that texture zeros can be enforced in arbitrary entries of the fermion mass matrices by means of Abelian symmetries (Grimus et al. 2004). In fact, it is possible to construct viable patterns in a minimal framework, i.e., with the smallest discrete Abelian group and a minimal number of Higgs scalars (Correia et al. 2019; González Felipe & Serôdio 2014; González Felipe & Serôdio 2017).

Flavor symmetries have also been used to address the so-called flavor hierarchy problem (or flavor puzzle) in the lepton sector. The main idea is to extend the SM symmetry group and use suitable representations for the lepton fields under a horizontal symmetry, i.e., a symmetry that acts on fields of different flavors. Several types of symmetries have been considered so far: Abelian or non-Abelian, continuous or discrete, and global or local (for a plethora of examples, see the reviews by Altarelli & Feruglio (2010), Ishimori et al. (2010), King & Luhn (2013)). Given the peculiar structure of the PMNS mixing matrix, when compared with its analogous CKM matrix, it is encouraging to impose a flavor symmetry to explain the mixing angles and CP-violating phases in the PMNS matrix, which otherwise would be arbitrary parameters. Flavor model building is a rapidly evolving research field and it is expectable that some classes of models will be ruled out by confronting their predictions with observational data, while others may remain as viable models, possibly distinguishable.

4 | CONCLUSIONS

Neutrino physics is an active and rich field of research, which currently benefits from the complementary information compiled from laboratory, cosmological, and astrophysical neutrino probes. Over the last decades, a remarkable progress has been made in understanding the properties of neutrinos. In this article, we have briefly covered several aspects of neutrino physics from the experimental and theoretical points of view.

From the topics presented here, we can conclude that the forthcoming years will be of utmost importance in elucidating the nature of neutrinos, the origin of their masses, and the way they interact. Laboratory searches for neutrino flavor oscillations, β-decay and $0\nu\beta\beta$-decay experiments, combined with observational data from astrophysical neutrino sources and cosmology, will undoubtedly play a crucial role along the pathway to a complete picture of the neutrino sector.

ACKNOWLEDGMENTS

The author acknowledges the support of Fundação para a Ciência e a Tecnologia (FCT, Portugal) through the projects CFTP-FCT Unit UIDB/00777/2020, UIDP/00777/2020, and CERN/FIS-PAR/0019/2021, which are partially funded through POCTI (FEDER), COMPETE, QREN, and EU.

CONFLICT OF INTEREST STATEMENT

The author declares no potential conflict of interests.

ORCID

Ricardo González Felipe https://orcid.org/0000-0003-3563-6626

REFERENCES

Aartsen, M. G., Ackermann, M., Adams, J., et al. 2018, *Phys. Rev. Lett.*, *120*(7), 071801.

Aartsen, M. G., Ackermann, M., Adams, J., et al. 2019, *Phys. Rev. D*, *99*(3), 032007.

Abazajian, K. N. 2017, *Phys. Rept.*, *711-712*, 1.

Abe, K., Haga, Y., Hayato, Y., et al. 2016, *Phys. Rev. D*, *94*(5), 052010.

Abe, K., Bronner, C., Hang, Y., et al. 2018a, *Phys. Rev. D*, *97*(7), 072001.

Abe, K., Abe Ke., Aihara, H., et al. 2018b. e-Print: 1805.04163.

Abe, K., Akutsu, R., Ali, A., et al. 2020, *Nature*, *580*(7803), 339 ([Erratum: Nature 583, E16 (2020)]).

Abe, S., Ebihara, T., Enomoto, S., et al. 2008, *Phys. Rev. Lett.*, *100*, 221803.

Abe, S., Asami, S., Eizuka, M., et al. 2023, *Phys. Rev. Lett.*, *130*(5), 051801.

Abgrall, N., Abramov, A., Abrosimov, N., et al. 2017, *AIP Conf. Proc.*, *1894*(1), 020027.

Abi, B., Acciarri, R., Acero, M. A., et al. 2020, *JINST*, *15*(08), T08008.

Abratenko, P., An, R., Anthony, J., et al. 2022, *Phys. Rev. Lett.*, *128*(24), 241801.

Abreu, Y., Amhis, Y., Arnold, L., et al. 2021, *JINST*, *16*(02), P02025.

Acero, M. A., Adamson, P., Aliaga, L., et al. 2019, *Phys. Rev. Lett.*, *123*(15), 151803.

Adams, D. Q., Alduino, C., Alfonso, K., et al. 2022, *Nature*, *604*(7904), 53.

Adey, D., An, F. P., Balantekin, A. B., et al. 2018, *Phys. Rev. Lett.*, *121*(24), 241805.

Aghanim, N., Akrami, Y., Ashdown, M., et al. 2020, *Astron. Astrophys.*, *641*, A6 ([Erratum: Astron.Astrophys. 652, C4 (2021)]).

Agostini, M., Araujo, G. R., Bakalyarov, A. M., et al. 2020, *Phys. Rev. Lett.*, *125*(25), 252502.

Agrawal, P., Bauer, M., Beacham, J., et al. 2021, *Eur. Phys. J. C*, *81*(11), 1015.

Aguilar-Arevalo, A. A., Brown, B. C., Bugei, L., et al. 2018, *Phys. Rev. Lett.*, *121*(22), 221801.

Aguilar-Arevalo, A., Auerbach, B., Burman, R. L., et al. 2001, *Phys. Rev. D*, *64*, 112007.

Aiello, S., Albert, A., Garre, S. A., et al. 2022, *Eur. Phys. J. C*, *82*(1), 26.

Ajimura, S., Botran, M., Choi, J. H., et al. 2021, *Nucl. Instrum. Meth. A*, *1014*, 165742.

Aker, M., Altenmuller, K., Amsbaugh, J.F., et al. 2021, *JINST*, *16*(08), T08015.

Aker, M., Beglarian, A., Behrens, J., et al. 2022, *Nature Phys.*, *18*(2), 160.

Albanese, V., Alves, R., Anderson, M.R., et al. 2021, *JINST*, *16*(08), P08059.

Albert, A., André, M., Anghinolfi, M., et al. 2019, *JHEP*, *06*, 113.

Albert, J. B., Anton, G., Arnquist, I. J., et al. 2018, *Phys. Rev. C*, *97*(6), 065503.

Alekhin, S., Altmannshofer, W., Asaka, T., et al. 2016, *Rept. Prog. Phys.*, *79*(12), 124201.

Alekseev, I., Belov, V., Brudanni, V., et al. 2018, *Phys. Lett. B*, *787*, 56.

Alimonti, G., Arpesella, C., Back, H., et al. 2009, *Nucl. Instrum. Meth. A*, *600*, 568.

Almazán, H., Bernard, L., Blanchet, A., et al. 2020, *Phys. Rev. D*, *102*(5), 052002.

Altarelli, G., & Feruglio, F. 2010, *Rev. Mod. Phys.*, *82*, 2701.

An, F., An, G., An, Q., et al. 2016, *J. Phys. G*, *43*(3), 030401.

Andriamirado, M., Balantekin, A. B., Band, H. R., et al. 2021, *Phys. Rev. D*, *103*(3), 032001.

Anton, G., Badhrees, I., Barbeau, P. S., et al. 2019, *Phys. Rev. Lett.*, *123*(16), 161802.

Armatol, A., Augier, C., Avignone, F.T., et al. 2022. In *Snowmass 2021*, (Seattle, USA), e-Print: 2203.08386.

Asaka, T., Hamaguchi, K., Kawasaki, M., & Yanagida, T. 1999, *Phys. Lett. B*, *464*, 12.

Asner, D. M., Bradley, R. F., de Viveiros, L., et al. 2015, *Phys. Rev. Lett.*, *114*(16), 162501.

Bak, G., Choi, J. H., Jang, H. I., et al. 2018, *Phys. Rev. Lett.*, *121*(20), 201801.

Baldini, A. M., Bao, Y., Baracchini, E., et al. 2016, *Eur. Phys. J. C*, *76*(8), 434.

Barinov, V. V., Cleveland, B. T., Danshin, S. N., et al. 2022, *Phys. Rev. Lett.*, *128*(23), 232501.

Barreiros, D. M., Felipe, R. G., & Joaquim, F. R. 2018, *Phys. Rev. D*, *97*(11), 115016.

Bellgardt, U., Otter, G., Eichler, R., et al. 1988, *Nucl. Phys. B*, *299*, 1.

Berryman, J. M., Nikita Blinov, Vedran Brdar, et al. 2022. In *Snowmass 2021*, (Seattle, USA), e-Print: 2203.01955.

Bilenky, S. M., & Pontecorvo, B. 1976a, *Lett. Nuovo Cim.*, *17*, 569.

Bilenky, S. M., & Pontecorvo, B. 1976b, *Yad. Fiz.*, *24*, 603.

Bonnet, F., Hirsch, M., Ota, T., & Winter, W. 2012, *JHEP*, *07*, 153.

Borgohain, H., & Borah, D. 2021, *J. Phys. G*, *48*(7), 075005.

Boyarsky, A., Drewes, M., Lasserre, T., Mertens, S., & Ruchayskiy, O. 2019, *Prog. Part. Nucl. Phys.*, *104*, 1.

Branco, G. C., Emmanuel-Costa, D., González Felipe, R., & Serôdio, H. 2009, *Phys. Lett. B*, *670*, 340.

Branco, G. C., Felipe, R. G., & Joaquim, F. R. 2012, *Rev. Mod. Phys.*, *84*, 515.

Buchmuller, W., Di Bari, P., & Plumacher, M. 2005a, *Annals Phys.*, *315*, 305.

Buchmuller, W., Peccei, R. D., & Yanagida, T. 2005b, *Ann. Rev. Nucl. Part. Sci.*, *55*, 311.

Cabibbo, N. 1963, *Phys. Rev. Lett.*, *10*, 531.

Capozzi, F., Di Valentino, E., Lisi, E., Marrone, A., Melchiorri, A., & Palazzo, A. 2021, *Phys. Rev. D*, *104*(8), 083031.

Cebola, L. M., Emmanuel-Costa, D., & Felipe, R. G. 2015, *Phys. Rev. D*, *92*(2), 025005.

Cheng, T. P., & Li, L.-F. 1980, *Phys. Rev. D*, *22*, 2860.

Chun, E. J., Cvetič, G., Dev, P. S. B., et al. 2018, *Int. J. Mod. Phys. A*, *33*(05n06), 1842005.

Correia, S. S., Felipe, R. G., & Joaquim, F. R. 2019, *Phys. Rev. D*, *100*(11), 115008.

Cowan, C. L., Reines, F., Harrison, F. B., Kruse, H. W., & McGuire, A. D. 1956, *Science*, *124*, 103.

Dasgupta, B., & Kopp, J. 2021, *Phys. Rept.*, *928*, 1.

Davidson, S., Nardi, E., & Nir, Y. 2008, *Phys. Rept.*, *466*, 105.

Davis, R. Jr., Harmer, D. S., & Hoffman, K. C. 1968, *Phys. Rev. Lett.*, *20*, 1205.

de Salas, P. F., Forero, D. V., Gariazzo, S., et al. 2021, *JHEP*, *02*, 71.

Dick, K., Lindner, M., Ratz, M., & Wright, D. 2000, *Phys. Rev. Lett.*, *84*, 4039.

Dolinski, M. J., Poon, A. W. P., & Rodejohann, W. 2019, *Ann. Rev. Nucl. Part. Sci.*, *69*, 219.

Drewes, M., Lasserre, T., Merle, A., et al. 2017, *JCAP*, *01*, 25.

Dunne, P. 2020, *Latest Neutrino Oscillation Results from T2K*, Zenodo. Plenary talk in the XXIX International Conference on Neutrino Physics and Astrophysics.

Eliezer, S., & Swift, A. R. 1976, *Nucl. Phys. B*, *105*, 45.

Emmanuel-Costa, D., & González Felipe, R. 2017, *Phys. Lett. B*, *764*, 150.

Esteban, I., Gonzalez-Garcia, M. C., Maltoni, M., Schwetz, T., & Zhou, A. 2020, *JHEP*, *09*, 178.

Farzan, Y., & Tortola, M. 2018, *Front. in Phys.*, *6*, 10.

Foot, R., Lew, H., He, X. G., & Joshi, G. C. 1989, *Z. Phys. C*, *44*, 441.

Formaggio, J. A., de Gouvêa, A. L. C., & Robertson, R. H. 2021, *Physics Reports*, *914*, 1.

Frampton, P. H., Glashow, S. L., & Yanagida, T. 2002, *Phys. Lett. B*, *548*, 119.

Fritzsch, H., & Minkowski, P. 1976, *Phys. Lett. B*, *62*, 72.

Fukuda, Y., Hayakawa, T., Ichihara, E., et al. 1998, *Phys. Rev. Lett.*, *81*, 1562.

Fukugita, M., & Yanagida, T. 1986, *Phys. Lett. B*, *174*, 45.

Fuller, G. M., Kusenko, A., Mocioiu, I., & Pascoli, S. 2003, *Phys. Rev. D*, *68*, 103002.

Gando, A., Gando, Y., Ichimura, K., et al. 2011, *Phys. Rev. D*, *83*, 052002.

Gastaldo, L., Blaum, K., Chrysalidis, K., et al. 2017, *Eur. Phys. J. ST*, *226*(8), 1623.

Gell-Mann, M., Ramond, P., & Slansky, R. 1979, *Conf. Proc. C*, *790927*, 315.

Gerbino, M., Grohs, E., Lattanzi, M., et al. 2022. In *Snowmass 2021*, (Seattle, USA), e-Print: 2203.07377.

Giachero, A., Alpert, B.K., Becker, D.T., et al. 2017, *JINST*, *12*(02), C02046.

Giudice, G. F., Peloso, M., Riotto, A., & Tkachev, I. 1999, *JHEP*, *08*, 14.

Giunti, C., & Kim, C. W. 2007, *Fundamentals of Neutrino Physics and Astrophysics*. Oxford University Press.

Giunti, C., Li, Y. F., Ternes, C. A., & Xin, Z. 2022, *Phys. Lett. B*, *829*, 137054.
Glashow, S. L. 1980, *NATO Sci. Ser. B*, *61*, 687.
Gomez-Cadenas, J. J. 2019, *Electroweak Interactions and Unified Theories*, Moriond EW 2019, 201.
González Felipe, R., Joaquim, F. R., & Nobre, B. M. 2004, *Phys. Rev. D*, *70*, 085009.
González Felipe, R., & Serôdio, H. 2014, *Nucl. Phys. B*, *886*, 75.
González Felipe, R., & Serôdio, H. 2017, *J. Phys. G*, *44*(6), 065002.
Grimus, W., Joshipura, A. S., Lavoura, L., & Tanimoto, M. 2004, *Eur. Phys. J. C*, *36*, 227.
Harigaya, K., Ibe, M., & Yanagida, T. T. 2012, *Phys. Rev. D*, *86*, 013002.
Himmel, A. 2020, *New Oscillation Results from the NOvA Experiment*, Zenodo. Plenary talk in the XXIX International Conference on Neutrino Physics and Astrophysics.
Hirsch, M., Srivastava, R., & Valle, J. W. F. 2018, *Phys. Lett. B*, *781*, 302.
Ishida, T. 2013, *15th International Workshop on Neutrino Factories*, Super Beams and Beta Beams, (Beijing, China).
Ishihara, A. 2021, *PoS, ICRC2019*, *358*, 1031.
Ishimori, H., Kobayashi, T., Ohki, H., Shimizu, Y., Okada, H., & Tanimoto, M. 2010, *Prog. Theor. Phys. Suppl.*, *183*, 1.
Kaether, F., Hampel, W., Heusser, G., Kiko, J., & Kirsten, T. 2010, *Phys. Lett. B*, *685*, 47.
King, S. F., & Luhn, C. 2013, *Rept. Prog. Phys.*, *76*, 056201.
Ko, Y. J., Kim, B.R., Kim, J.Y., et al. 2017, *Phys. Rev. Lett.*, *118*(12), 121802.
Kobayashi, M., & Maskawa, T. 1973, *Prog. Theor. Phys.*, *49*, 652.
Konetschny, W., & Kummer, W. 1977, *Phys. Lett. B*, *70*, 433.
Kusenko, A., & Segre, G. 1997, *Phys. Lett. B*, *396*, 197.
Kuzmin, V. A., Rubakov, V. A., & Shaposhnikov, M. E. 1985, *Phys. Lett. B*, *155*, 36.
Lattanzi, M., Gerbino, M., Freese, K., Kane, G., & Valle, J. W. F. 2020, *JHEP*, *10*, 213.
Lazarides, G., Shafi, Q., & Wetterich, C. 1981, *Nucl. Phys. B*, *181*, 287.
Lee, M. H. 2020, *JINST*, *15*(08), C08010.
Loredo, T. J., & Lamb, D. Q. 2002, *Phys. Rev. D*, *65*, 063002.
Ludl, P. O., & Grimus, W. 2014, *JHEP*, *07*, 90 ([Erratum: JHEP 10, 126 (2014)]).
Ma, E. 2006, *Phys. Rev. D*, *73*, 077301.
Ma, E., & Popov, O. 2017, *Phys. Lett. B*, *764*, 142.
Maki, Z., Nakagawa, M., & Sakata, S. 1962, *Prog. Theor. Phys.*, *28*, 870.
Mention, G., Fechner, M., Lasserre, T., Mueller, T. A., Lhuillier, D., Cribier, M., & Letourneau, A. 2011, *Phys. Rev.D*, *83*, 073006.
Minkowski, P. 1977, *Phys. Lett. B*, *67*, 421.
Miranda, O. G., Tortola, M. A., & Valle, J. W. F. 2006, *JHEP*, *10*, 8.
Mohapatra, R. N. 1986, *Phys. Rev. Lett.*, *56*, 561.
Mohapatra, R. N., Antusch, S., Babu, K. S., et al. 2007, *Rept. Prog. Phys.*, *70*, 1757.
Mohapatra, R. N., & Senjanovic, G. 1980, *Phys. Rev. Lett.*, *44*, 912.
Mohapatra, R. N., & Senjanovic, G. 1981, *Phys. Rev. D*, *23*, 165.
Mohapatra, R. N., & Valle, J. W. F. 1986, *Phys. Rev. D*, *34*, 1642.
Mueller, T. A., Lhuillier, D., Fallot, M., et al. 2011, *Phys. Rev. C*, *83*, 054615.
Nakamura, R., Sambonsugi, H., Shiraishi, K., & Wada, Y. 2020, *J. Phys. Conf. Ser.*, *1468*(1), 012256.
Nunokawa, H., Parke, S. J., & Valle, J. W. F. 2008, *Prog. Part. Nucl. Phys.*, *60*, 338.
Pagliaroli, G., Rossi-Torres, F., & Vissani, F. 2010, *Astropart. Phys.*, *33*, 287.
Pilaftsis, A., & Underwood, T. E. J. 2004, *Nucl. Phys. B*, *692*, 303.
Pontecorvo, B. 1957, *Sov. Phys. JETP*, *6*, 429.
Sajjad Athar, M., Barwick, S.W., Brunner, T., et al. 2022, *Prog. Part. Nucl. Phys.*, *124*, 103947.
Sakharov, A. D. 1967, *Pisma Zh. Eksp. Teor. Fiz.*, *5*, 32.
Schechter, J., & Valle, J. W. F. 1980, *Phys. Rev. D*, *22*, 2227.
Serebrov, A. P., Samoilov, R.M., Ivochkin, V.G., et al. 2021, *Phys. Rev. D*, *104*(3), 032003.
't Hooft, G. 1976, *Phys. Rev. Lett.*, *37*, 8.
't Hooft, G. 1980, *NATO Sci. Ser. B*, *59*, 135.
Turzynski, K. 2004, *Phys. Lett. B*, *589*, 135.
Weinberg, S. 1979, *Phys. Rev. Lett.*, *43*, 1566.
Workman, R. L., Burkert, V. D., Crede, V., et al. 2022, *Prog. Theor. Exp. Phys.*, *2022*, 083C01.
Yanagida, T. 1979, *Conf. Proc. C*, *7902131*, 95.
Zee, A. 1980, *Phys. Lett. B*, *93*, 389 ([Erratum: Phys.Lett.B 95, 461 (1980)]).
Zhao, J., Wen, L.-J., Wang, Y.-F., & Cao, J. 2017, *Chin. Phys. C*, *41*(5), 053001.

AUTHOR BIOGRAPHY

Ricardo González Felipe obtained his PhD in Physics from Helsinki University in 1994. He is a professor at Instituto Superior de Engenharia de Lisboa (ISEL) and a permanent member of the Centre for Theoretical Particle Physics (CFTP). His research covers different topics of particle physics and cosmology, including the matter-antimatter asymmetry of the Universe, CP violation and neutrino physics.

How to cite this article: Felipe, R. G. 2023, *Astron.Nachr./AN*, *344*, e230095. https://doi.org/10.1002/asna.20230095